01

Analytical solution for the populations of the energy levels of alkali metals under optical pumping and mixing of excited state sublevels

© F.S. Sviridov[1,2], A.K. Vershovskii[1]¶

[1] Ioffe Institute, St. Petersburg, Russia
[2] Alferov Federal State Budgetary Institution of Higher Education and Science Saint Petersburg National Research Academic University of the Russian Academy of Sciences, St. Petersburg, Russia

¶ e-mail: antver@mail.ioffe.ru

Received November 29, 2024
Revised November 29, 2024
Accepted December 12, 2024

The paper presents the results of an analytical calculation of the system of balance equations describing the populations of the energy levels of the ground state and the total population of the excited state of alkali metals under optical pumping under conditions when collisions with a buffer gas cause complete mixing of the sublevels of the excited state. This situation is realized in a number of quantum sensors, such as frequency standards, gyroscopes, magnetometers, using a cell with alkali metal vapor and a buffer inert gas as a sensitive element. A comparison with the experiment is given. The results can be used for spectroscopic non-destructive testing of the gas composition of such cells.

Keywords: optically detected magnetic resonance, optical pumping, relaxation.

DOI: 10.61011/EOS.2024.12.60448.7375-24

Introduction

Among quantum optical sensors the special place by their prevalence and variety belongs to the sensors based on various modifications of the optically detected magnetic resonance (ODMR) in the ground state of alkali metals. Development of compact sources of laser pumping such as semiconductor lasers with distributed feedback, and then with vertical cavities enabled development of miniature optical quantum sensors [1], such as microscale frequency standards [2,3], quantum magnetometers [4–8] and rotation sensors or gyroscopes [9,10]. The main sensitive element in all of these devices is a transparent cell containing alkali metal atoms, as well as a buffer inert gas or a mixture of inert gases, slowing down the diffusion of atoms to the cell walls, and, accordingly, relaxation of sublevels of the alkali metal ground state.

One of the most complicated tasks in production of miniature quantum sensors is to make cells with strictly maintained pressures of the gas mixture components [11,12] and do their non-destructive testing, which after cell sealing (tapping) may only be done with spectroscopic means [13,14]. Each buffer gas causes spectral absorption lines shift and broadening that are unique to it, therefore study of these parameters in case of one- or two-component gas mixture may provide the complete information on its composition [15].

This method suggests scanning of the laser light frequency in the vicinity of D_1- or D_2-absorption lines and detection of absorption in the cell. In this case, the parameters of the absorption line turn out to be distorted by the processes of optical (firstly, hyperfine) pumping: to bleach the medium with hyperfine optic pumping, the intensity that is lower by many orders is required compared to the bleaching that is „traditional“ for the optical spectroscopy due to saturation of the optical transition. The bleaching value at the same time turns out to be frequency-dependent, which causes distortions of the spectral line contour. The accounting for these distortions requires calculation of populations in the conditions of presence of the optic pumping and buffer gas. Such calculations were done many times, starting from the fundamental papers [16–18] and until recently [19–21]; the solution to the specific task for ^{87}Rb is given in [22]. This paper presents a simple model for such calculation and its universal, i.e. valid for any alkali metal, analytical solutions.

Theory

As we have already mentioned, the working cells contains alkali metal atoms and the buffer inert gas (or a mix of inert gases), which moderates the wall relaxation. The exchange of spin states between metal atoms becomes the mechanism governing relaxation in this case. Since the cross sections of collision with atoms (molecules) of buffer gas for the excited states exceed by many orders the cross sections for the ground state, the cells with buffer gases or gas mixtures already at the pressures of around 3−10 Torr demonstrate the so called mixing of excited state sublevels — for the time when the atom stays in the excited state, populations of this state sublevels manage to balance themselves through collisions [18]. As a result the velocities of ground state sublevel occupation become identical (it is easy to confirm that by summing the probabilities of transitions to each

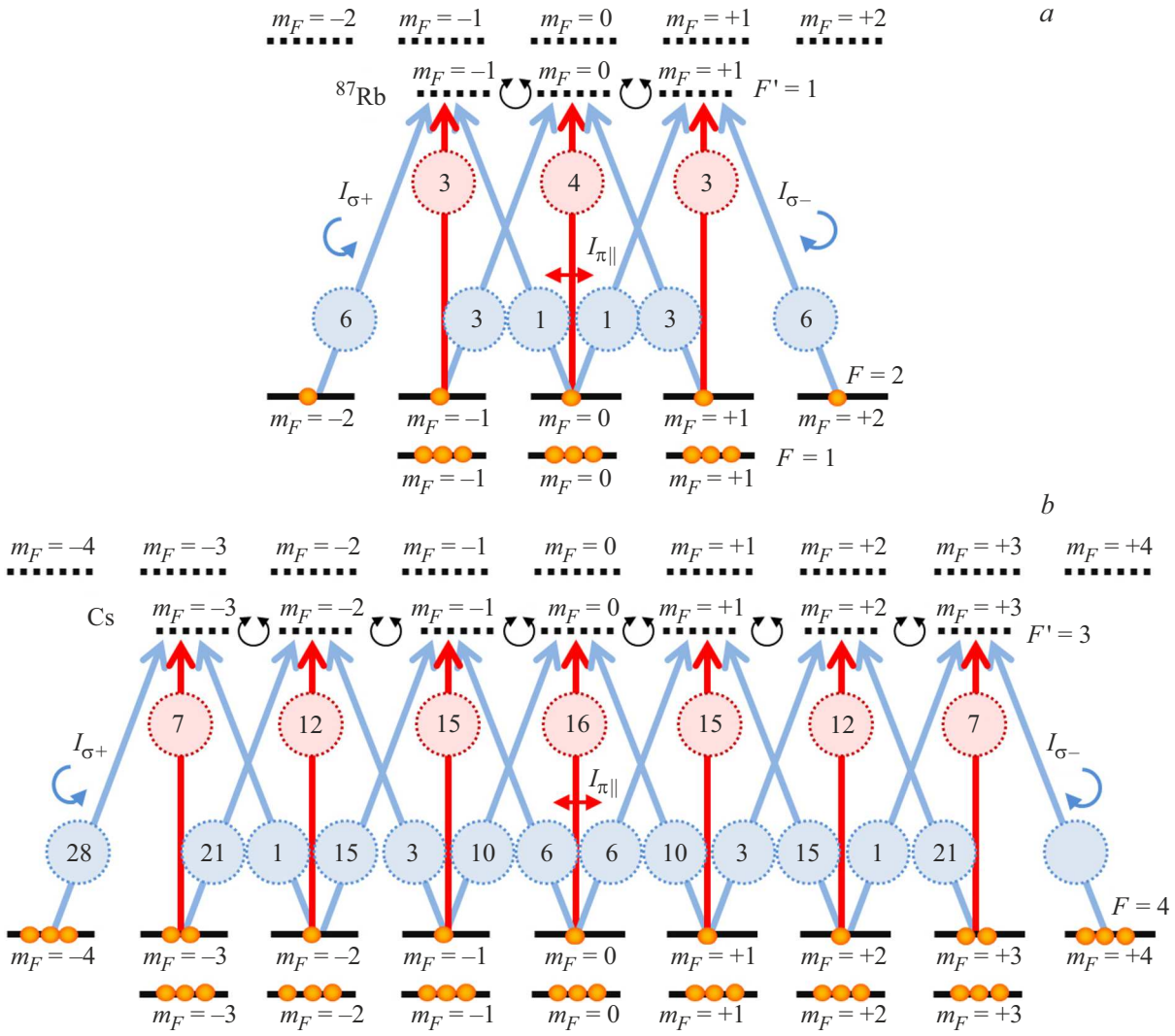

Figure 1. Schemes of Zeeman sublevels of the ground state of alkali metal atoms: (*a*) rubidium ^{87}Rb and (*b*) Cs. Digits on the arrows indicate relative probabilities of excitation under the effect of light with circular (σ^+, σ^-) and linear ($\pi_\|$, $\mathbf{E} \parallel \mathbf{B}$) polarizations, resonant to transition $F = I + 1 \to F' = I - 1$.

sublevel of the ground state from all sublevels of the excited state, see below), and the difference of their occupations is only caused by the difference in the velocities of optical excitation — the so called („depopulation pumping“).

Let us consider (fig. 1) the scheme of sublevels of the alkali metal atom ground state with nuclear spin $I = 3/2$. Such atoms include ^{7}Li, ^{23}Na, ^{39}K, ^{41}K, ^{87}Rb. Most frequently the schemes of quantum sensors use atom ^{87}Rb, and further we will mean this atom as the alkali metal atom. The next by the degree of utilization in the quantum sensorics are the cesium atoms Cs with nuclear spin $I = 7/2$, ^{87}Rb ($I = 5/2$) and potassium isotopes ^{39}K and ^{41}K ($I = 3/2$). The solutions for them are found in a similar way. Every hyperfine level $F = I \pm 1/2$ of the main ($S_{1/2}$) and excited ($P_{1/2}$) states in the magnetic field is split into $2F + 1$ magnetic (or Zeeman) sublevels with projections of moment $m_F = -F,\ F + 1,\ \ldots,\ F - 1,\ F$. The total number of these sublevels is $N = 2(2I + 1)$, accordingly in case of ^{87}Rb $N = 8$. At room temperature the Zeeman sublevels of the ground state are occupied evenly, since the hyperfine splitting of the ground state $5S_{1/2}$ for ^{87}Rb (6.8 GHz) and $6S_{1/2}$ for Cs (9.2 GHz) in the energy scale does not exceed 10^{-3} of the thermal energy kT. Due to mixing of excited state sublevels they may be considered as one level with population n_e and decay velocity Γ. As a result we obtain the system of $N + 1$ linear balance equations for occupations of type

$$\begin{cases} \frac{d}{dt} n_i = -p_i n_i - \gamma n_i + \frac{\gamma}{N} \sum\limits_{i=1}^{N} n_i + \frac{\Gamma}{N} n_e = 0, \\ \frac{d}{dt} n_e = -\Gamma n_e + \sum\limits_{i=1}^{N} p_i n_i = 0, \end{cases} \tag{1}$$

where $i = 1,\ 2,\ \ldots,\ N$, n_i — populations of Zeeman sublevels of the ground state, γ — dark (i. e. measured in the absence of pumping light) velocity of relaxation in

Table 1. Optical pumping velocity coefficients C_i for magnetic sublevels of the ground state of rubidium atoms ^{87}Rb when pumped with light of D_1-line with subsequent polarizations: circular σ^+, circular σ^-, linear $\pi_\parallel$ ($\mathbf{E} \parallel \mathbf{B}$), linear $\pi_\perp$ ($\mathbf{E} \perp \mathbf{B}$). For clarity of the representation the values were multiplied by a common denominator k

$F \to F'$	m_F	$F' = 1$				$F' = 2$			
		σ^+	σ^-	$\pi_\parallel$	$\pi_\perp$	σ^+	σ^-	$\pi_\parallel$	$\pi_\perp$
$F = 1$	−1	0	5	5	2.5	6	1	3	3.5
	0	5	5	0	5	3	3	4	3
	1	5	0	5	2.5	1	6	3	3.5
k		10				10			
$F = 2$	−2	0	6	0	3	0	2	4	1
	−1	0	3	3	1.5	2	3	1	2.5
	0	1	1	4	1	3	3	0	3
	1	3	0	3	1.5	3	2	1	2.5
	2	6	0	0	3	2	0	4	1
k		10				10			

the ground state, $p_i \sim C_i P(\omega) I_p$ — velocity of optical depumpung from level i, ω — light frequency, I_p — intensity of pumping light, $P(\omega)$ — distribution corresponding to the shape of the absorption line, coefficients C_i are proportional to the squares of the modules of the dipole matrix elements: $C_i \sim |d_{fi}|^2$.

Values of coefficients C_i for all possible transitions of D_1-line in atom ^{87}Rb are given in table 1, in Cs atom — in table 2. These values may be calculated up to a constant using formula

$$|d_{fi}| \sim \sqrt{2F_1 + 1} \begin{Bmatrix} I & J_1 & F_1 \\ 1 & F_2 & J_2 \end{Bmatrix} C^{F_2 m_{F2}}_{F_1 m_{F1} 1 p}, \qquad (2)$$

where $p = 0, \pm 1$ — polarization, I — nuclear spin of the atom, J — full electron moment, F — full atom moment, indices 1, 2 mean the initial and final states, accordingly. The formula uses $6j$-symbols and Clebsch−Gordan coefficients [23,24]. Value $p = 0$ corresponds to $\pi_\parallel$-polarization of light (linear with azimuth parallel to the field), values $p = -1$ and $p = +1$ — to circular polarizations σ^- ($\Delta m_F = -1$) and σ^+ ($\Delta m_F = +1$) accordingly.

In fig. 2 the optical pumping velocity coefficients C_i given in tables 1 and 2, are presented graphically. It can be seen from the graphs that in all the considered cases the effect of optical pumping is absent when the intensities of radiations with circular σ^+ and σ^- are equal (accordingly, the sum of these radiations is a linearly polarized radiation with intensity $I_{\pi\perp} = I_{\sigma^+} + I_{\sigma^-} = 2I_{\sigma^+} = 2I_{\sigma^-}$), and each of these intensities is equal to intensity of radiation with linear $\pi_\parallel$-polarization ($I_{\sigma^+} = I_{\sigma^-} = I_{\pi\parallel}$), from which $I_{\pi\perp} = 2I_{\pi\parallel}$ follows. This condition is met when pumped with linearly polarized radiation, the plane of polarization of which is located at angle $\varphi_M = \arccos(1/\sqrt{3})$ to magnetic field (so called „magic angle“ [25]). As the value of the magnetic moment increases, as well as the number of the involved sublevels, the coefficients approach the classic limit.

In equations (1) the first summand describes the depopulation pumping under action of light, the second and third ones — the spin relaxation of the ground state sublevels, the fourth one — relaxation of the excited state that is considered as one level without the hyperfine structure. If all equations (1) are summed up, we will get the condition for conservation of the number of atoms in the system

$$\frac{d}{dt}\left(\sum_{i=1}^{N} n_i + n_e\right) = 0. \qquad (3)$$

Let us accept the following condition of normalization:

$$\sum_{i=1}^{N} n_i + n_e = 1. \qquad (4)$$

The direct solution for the system (1) with the increase in the number of levels becomes more and more complicated and bulky. Already for $N = 3$ and $i = 1$ it looks as follows:

$$n_1 = \frac{\Gamma(\gamma + p_2)(\gamma + p_3)}{\Gamma p_1 p_2 + 3 p_1 p_2 p_3 + \Gamma(p_1 + p_2) p_3 + \gamma^2(3\Gamma + p_1 + p_2 + p_3) + 2\gamma(p_1 p_2 + (p_1 + p_2) p_3 + \Gamma(p_1 + p_2 + p_3))}. \qquad (5)$$

Nevertheless, this solution may be substantially simplified and recorded in the form common for any i and N. If designations $W_i = p_i + \gamma$ are entered (full velocity of atom exit from level i) and $\tau_i = 1/W_i$ (lifetime of level i), and also A (average weighted velocities p_i with weights τ_i):

$$A = \sum_{i=1}^{N} \frac{p_i}{W_i} \left(\sum_{j=1}^{N} \frac{1}{W_j}\right)^{-1} = \frac{\Sigma_i (p_i \tau_i)}{\Sigma_j \tau_j}, \qquad (6)$$

Table 2. Optical pumping velocity coefficients C_i for magnetic sublevels of the ground state of rubidium atoms ^{87}Rb when pumped with light of D_1-line with subsequent polarizations: circular σ^+, circular σ^-, linear $\pi_\parallel$ ($\mathbf{E} \parallel \mathbf{B}$), linear $\pi_\perp$ ($\mathbf{E} \perp \mathbf{B}$). For clarity of the representation the values were multiplied by a common denominator k

$F \to F'$	m_F	$F' = 3$				$F' = 4$			
		σ^+	σ^-	$\pi_\parallel$	$\pi_\perp$	σ^+	σ^-	$\pi_\parallel$	$\pi_\perp$
$F = 3$	-3	0	3	9	1.5	28	1	7	14.5
	-2	3	5	4	4	21	3	12	12
	-1	5	6	1	5.5	15	6	15	10.5
	0	6	6	0	6	10	10	16	10
	1	6	5	1	5.5	6	15	15	10.5
	2	5	3	4	4	3	21	12	12
	3	3	0	9	1.5	1	28	7	14.5
k		$7 \times 4 = 28$				$21 \times 4 = 84$			
$F = 4$	-4	0	28	0	14	0	4	16	2
	-3	0	21	7	10.5	4	7	9	5.5
	-2	1	15	12	8	7	9	4	8
	-1	3	10	15	6.5	9	10	1	9.5
	0	6	6	16	6	10	10	0	10
	1	10	3	15	6.5	10	9	1	9.5
	2	15	1	12	8	9	7	4	8
	3	21	0	7	10.5	7	4	9	5.5
	4	28	0	0	14	4	0	16	2
k		$21 \times 4 = 84$				$15 \times 4 = 60$			

the solution to system (1) will be

$$n_i = \frac{\Gamma}{A+\Gamma}\frac{\tau_i}{\Sigma_j \tau_j},$$

$$n_e = \frac{A}{A+\Gamma}. \tag{7}$$

The produced solution may easily be tested by substitution in the initial system: using the normalization condition (4), let us substitute sum $\sum\limits_i n_i = 1 - n_e$ in the first N equations of system (1), then we substitute n_i and n_e (7), the right parts of the equations will look like

$$-\frac{\Gamma}{A+\Gamma}(p_i+\gamma)\frac{\tau_i}{\Sigma_j \tau_j} + \frac{\Gamma}{A+\Gamma}\frac{A+\gamma}{N}, \tag{8}$$

where by definition $(p_i + \gamma)\tau_i = 1$, and then

$$A + \gamma = \frac{\Sigma_i (p_i \tau_i)}{\Sigma_j \tau_j} + \gamma = \frac{\Sigma_i (p_i + \gamma)\tau_i}{\Sigma_j \tau_j} = \frac{N}{\Sigma_j \tau_j}. \tag{9}$$

This provides for equality of expression (8) to zero, the last equality of the system is also easily tested by direct substitution of values (7).

In cells with the alkali metal vapors the ratio Γ/γ depending on the buffer gas pressure may be $\Gamma/\gamma \sim 10^5 - 10^7$. Therefore, we may assume that in the cells with thermal atoms $\Gamma/\gamma \gg 1$. Since the optimization of the quantum sensor parameters requires compliance with condition $p_i \sim k\gamma$, where $k = 3-5$ [26], we may also assume that $\Gamma/A \gg 1$ — in cells of any size used in practice this is fair for all technically achievable capacities of the laser pumping. Then solution (7) is reduced to

$$n_i \sim \frac{\tau_i}{\Sigma_j \tau_j},$$

$$n_e \sim 0. \tag{10}$$

Thus, in the absence of taking into account the finite relaxation time of the excited state the result is simplified to the maximum: the population of every level in pure „de-pumping“ is equal to the ratio of the lifetime of this level to the sum of all levels.

Fig. 3 and 4 show the dependences of the rubidium ^{87}Rb atom ground state level populations on intensity of light I/γ, calculated as per (7) accordingly for the left circular polarization and for the linear polarization parallel to the magnetic field.

Let us also consider the limit case of strong intensity of pumping light ($\Sigma p_i/N \gg \gamma$). Let the light of σ^+-polarization be incident on the system. In this case there is the only Zeeman sublevel i_0, not interacting with optical pumping — for ^{87}Rb it is sublevel $m_F = 2$, for which the corresponding velocity is $C_{i0} = 0$. Accordingly, one may expect that most atoms will be exactly in this state. In the extreme case $I \to \infty$ this quantity will depend on the ratio of relaxation of the excited state to dark relaxation, Γ/γ. By

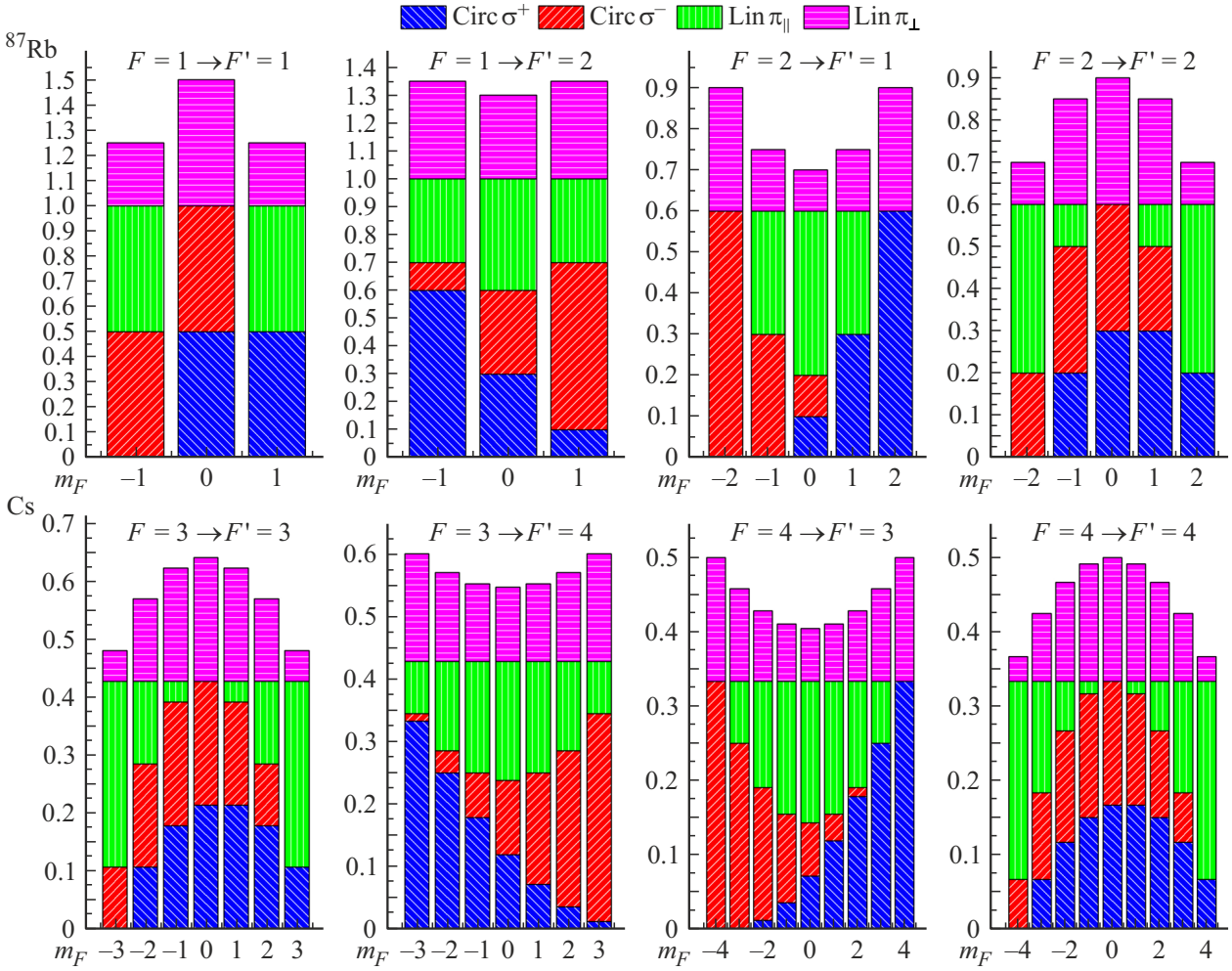

Figure 2. Diagrams of optical pumping velocity coefficients C_i in Tables 1 and 2 for magnetic sublevels of the ground state of rubidium atoms ^{87}Rb and cesium Cs when pumped with light of D_1-line with subsequent polarizations: circular σ^+, circular σ^-, linear $\pi_{\|}$ ($\mathbf{E} \parallel \mathbf{B}$), linear ($\mathbf{E} \perp \mathbf{B}$).

carrying out the limit transition $I \to \infty$ in the expressions for populations (7), we find

$$n_i = \frac{\Gamma}{(N-1)\gamma + \Gamma}\delta_{i,i_0},$$
$$n_e = \frac{(N-1)\gamma}{(N-1)\gamma + \Gamma}. \qquad (11)$$

In cells with alkali metal vapors and buffer gas $\Gamma/\gamma \gg 1$ and $n_{i0} \approx 1$.

Experiment

The obtained dependences were tested by us experimentally. For this purpose the absorption profiles were measured in the cell containing rubidium ^{87}Rb and ~ 30 Torr buffer gas vapors (mix of Ar and Ne), in the vicinity of D_1-absorption line. A semiconductor laser with an external cavity produced by VitaWave (Troitsk, Moscow) was used. Since the absorption contours corresponding to transitions from one hyperfine level of the ground state are poorly resolved (insert in fig. 5), we compared the experimentally measured integral absorption (total area of contours $F = 2 \to F = 1, 2$) with the calculation result by (7) and (12):

$$\int K(\omega)d\omega = \int \sum_{i=1}^{N} C_i n_i(\omega)d\omega. \qquad (12)$$

At the same time the effects of hyperfine pumping that distort the contour were taken into account (fig. 4). In process of comparison the theoretical curve was adjusted by intensity parameter.

Figure 5 demonstrates good agreement of theory and the experiment. Excessive spread of dots is caused by the error of basic line definition under the conditions of the final range of continuous tuning of the laser. Note that such agreement with the experiment may not be obtained for each individual contour.

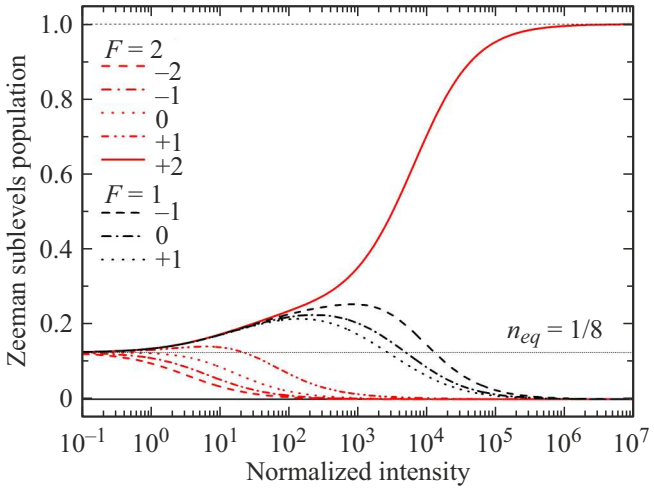

Figure 3. Populations of rubidium ^{87}Rb atom levels depending on light intensity. Optical pumping is circularly polarized (σ^+-polarization), the pumping light frequency is resonant to low-frequency transition $F = 2 \to F' = 1$, distribution $P(\omega)$ is considered to be Lorentz with width $\gamma_L = 400$ MHz. Light intensity is normalized by velocity of „dark" relaxation γ, ratio $\Gamma/\gamma = 10^6$.

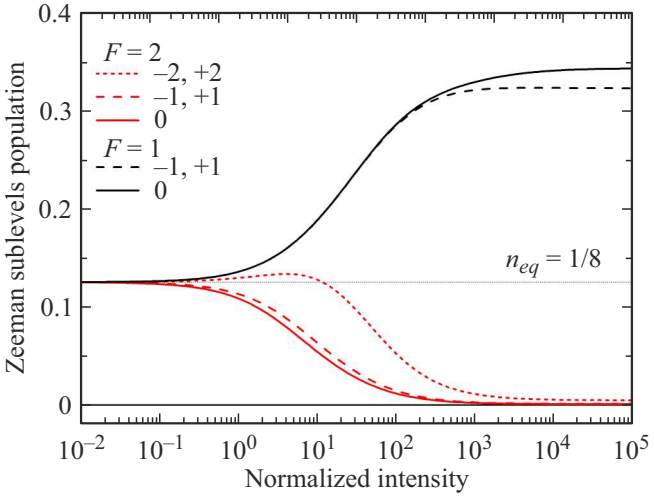

Figure 4. Populations of rubidium ^{87}Rb levels depending on light intensity. Azimuth of linear polarization of optical pumping is parallel to magnetic field ($\pi_\parallel$-polarization), the other parameters are the same as in fig. 3.

Conclusions

We obtained the analytical solution to the system of linear balance equations for the levels populations — common for any quantity and, therefore, any values of nuclear spin I, i. e. for any alkali metals. The obtained solution was tested by comparison with the experiment done in cell with ^{87}Rb. The results may be used to calculate the spectral characteristics of absorption in the cells of miniature quantum sensors, including in the spectroscopic non-destructive testing of the gas composition of such cells.

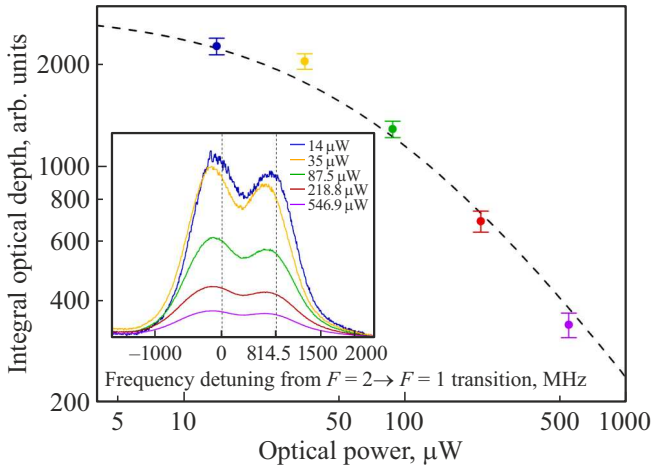

Figure 5. Optical density of rubidium ^{87}Rb vapors in the vicinity of D_1-line of absorption in the cell, containing ~ 30 Torr of buffer gas (mix of Ar and Ne), depending on light intensity. Solid line — theory, dots — experiment. In the insert — contours of absorption at intensities corresponding to experimental dots in the curve.

Funding

This study was financed within the framework of the project FFUG-2024-0039 of Ioffe Institute.

Conflict of interest

The authors declare that they have no conflict of interest.

References

[1] C.L. Degen, F. Reinhard, P. Cappellaro. Rev. Mod. Phys., **89** (3), 035002 (2017). DOI: 10.1103/RevModPhys.89.035002
[2] S. Knappe, P. Schwindt, V. Shah, L. Hollberg, J. Kitching, L. Liew, J. Moreland. Opt. Express, **13** (4), 1249 (2005). DOI: 10.1364/OPEX.13.001249
[3] J. Kitching. Appl. Phys. Rev., **5** (3), 238 (2018). DOI: 10.1063/1.5026238
[4] D. Budker, M. Romalis. Nature Physics, **3**, 227 (2007). DOI: 10.1038/nphys566
[5] T.H. Sander, J. Preusser, R. Mhaskar, J. Kitching, L. Trahms, S. Knappe. Biomed. Opt. Express, **3** (5), 981 (2012). DOI: 10.1364/BOE.3.000981
[6] H. Korth, K. Strohbehn, F. Tejada, A.G. Andreou, J. Kitching, S. Knappe, S.J. Lehtonen, S.M. London, M. Kafel. J. Geophys. Res. Space Physics, **121** (8), 7870 (2016). DOI: 10.1002/2016JA022389
[7] E. Boto, N. Holmes, J. Leggett, G. Roberts, V. Shah, S.S. Meyer, L.D. Muñoz, K.J. Mullinger, T.M. Tierney, S. Bestmann, G.R. Barnes, R. Bowtell, M.J. Brookes. Nature, **555**, 657 (2018). DOI: 10.1038/nature26147
[8] O. Alem, K.J. Hughes, I. Buard, T.P. Cheung, T. Maydew, A. Griesshammer, K. Holloway, A. Park, V. Lechuga, C. Coolidge et al. Frontiers in Neuroscience, **17**, 1014 (2023). DOI: 10.3389/fnins.2023.1190310

[9] D. Meyer, M. Larsen. Gyroscopy and Navigation, **5** (2), 75 (2014). DOI: 10.1134/S2075108714020060
[10] A.K. Vershovskii, Yu.A. Litmanovich, A.S. Pazgalev, V.G. Peshekhonov. Gyroscopy and Navigation, **9** (3), 162 (2018). DOI: 10.1134/S2075108718030100.
[11] O. Kozlova, S. Guérandel, E. de Clercq. Phys. Rev. A, **83** (6), 062714 (2011). DOI: 10.1103/PhysRevA.83.062714
[12] N. Almat, M. Gharavipour, W. Moreno, F. Gruet, C. Affolderbach, G. Mileti. IEEE Transactions on Ultrasonics, Ferroelectrics, and Frequency Control, **67** (1), 207 (2020). DOI: 10.1109/TUFFC.2019.2940903
[13] G.A. Pitz, A.J. Sandoval, T.B. Tafoya, W.L. Klennert, D.A. Hostutler. JQSRT, **140**, 18 (2014). DOI: 10.1016/j.jqsrt.2014.01.024
[14] A. Andalkar, R.B. Warrington. Phys. Rev. A, **65** (3), 032708 (2002). DOI: 10.1103/PhysRevA.65.032708
[15] J. Peng, Z. Liu, K. Yin, S. Zou, H. Yuan J. Phys. D, **55** (36), 365005 (2022). DOI: 10.1088/1361-6463/ac73c0
[16] F.A. Franz. Phys. Rev., **141** (1), 105 (1966). DOI: 10.1103/PhysRev.141.105
[17] F.A. Franz, J.R. Franz. Phys. Rev., **148** (1), 82 (1966). DOI: 10.1103/PhysRev.148.82
[18] W. Happer. Rev. Mod. Phys., **44** (2), 169 (1972). DOI: 10.1103/RevModPhys.44.169
[19] E.N. Popov, V.A. Bobrikova, S.P. Voskoboinikov, K.A. Barantsev, S.M. Ustinov, A.N. Litvinov, A.K. Vershovskii, S.P. Dmitriev, V.A. Kartoshkin, A.S. Pazgalev, M.V. Petrenko. JETP Letters, **108** (8), 513 (2018). DOI: 10.1134/S0021364018200122.
[20] K.A. Barantsev, E.N. Popov, A.N. Litvinov. Quant. Electron., **47** (9), 812 (2017). DOI: 10.1070/QEL16447.
[21] A. Van Lange, P. Van der Straten, D. Van Oosten. J. Phys. B, **53** (12), 125402 (2020). DOI: 10.1088/1361-6455/ab7fc2
[22] A.K. Vershovskii, A.S. Pazgalev, F.S. Sviridov. Opt. Spectrosc. **132** (12), 1210–1213 (2024).
[23] I.I. Sobelman. *Atomic Spectra and Radiative Transitions*, vol. 12 (Springer Science & Business Media, 2012).
[24] D. Varshalovich, A. Moskalev, V. Khersonskii. *Quantum Theory of Angular Momentum* (World scientific, 1988).
[25] S. Schott, A. Steinbacher, J. Buback, P. Nuernberger, T. Brixner. J. Phys. B, **47** (12), 124014 (2014). DOI: 10.1088/0953-4075/47/12/124014
[26] A.K. Vershovskii, A.S. Pazgalev. Technical Physics, **53** (5), 646 (2008). DOI: 10.1134/S1063784208050198.

Translated by M.Verenikina